A NEW ELECTROMAGNETIC IMAGING SCHEME①

Zhang Rongfeng, He Jishan
College of Resource, Environment and Civil Engineering,
Central South University of Technology, Changsha 410083

ABSTRACT A new electromagnetic imaging scheme, including equipment, setting and image algorithm, was put forward. The surface-to-well setting, with an alternating current source on the surface, was adopted. A new two step inversion algorithm, namely inverse scattering current at first and then inverse electric conductivity, was employed. Through this method, the difficult nonlinear image equations are linearized, so electromagnetic imaging for any kind of electric conductivity contrasts can be done principally.

Key words electromagnetic imaging born approximation inversion

1 INTRODUCTION

Electromagnetic imaging has important and potential values in detail survey of metallic ore deposit, environment monitoring and oil extraction, etc. At present there exist some complete schemes, including equipment, survey and inverse algorithm[1]. However, because of the natural characteristics of electromagnetic wave such as diffusion, these schemes are not satisfactory and difficult to carry out. Crosswell setting is usually employed, and the inverse algorithms are many kinds of Born approximation iteration scheme[1-4]. Since Born approximation is used, these algorithms are only suitable to geology bodies with small contrast of electric properties. Unfortunately, this condition is hard to be satisfied. Although Habashy (1993) put forward a modified approximation method[5], which was used in electromagnetic imaging by Torres-Verdin (1993)[6], this might decrease the request of contrast slightly. For this reason, we suppose a simple algorithm without any approximation.

2 VERTICAL ELECTRICITY PROFILE

For convenience, we call our scheme as VEP, that is, vertical electricity profile (vs VSP in seismic). See Fig. 1, an electric dipole source or a long horizontal electricity wire source is located on the surface, and there is only one well, which is located on the equator plane of the source. Measurements are carried out along the surface and along the well, H_z and H_x may be recorded in well; H_x, H_z and E_y may be recorded on the surface. For simple cases, we record H_z in well and record H_x and or E_y on the surface. There are two main advantages about this scheme: the first is only one well is needed which is easier to fit to the field conditions; the second is that it is convenient to supply current by wire on the surface and there are currently available services, and the more important is that powerful exciting signal can be supplied in this

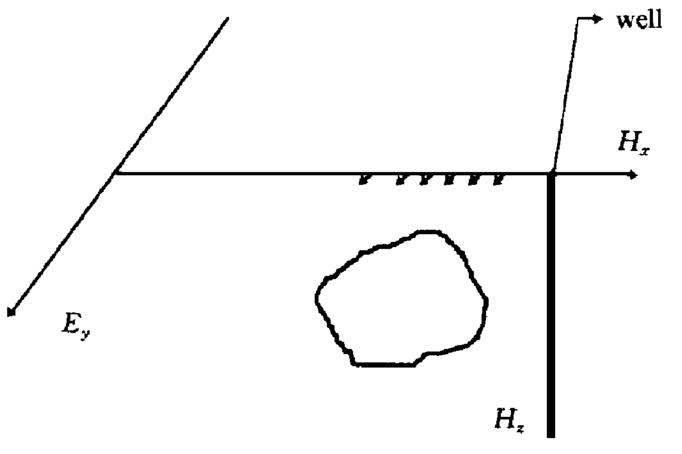

Fig. 1 VEP geometry

① Supported by the National Doctorate Program Fund of State Education Committee of China

Received Jul. 29, 1996; accepted Jan. 14, 1997

manner, so that increase signal-to-noise ratio, decrease the request to the receiver system. However, it is hard to do in well.

3 IMAGING ALGORITHM

We consider 2D structure, and assume the source is a long infinite current source. Then, the primary field and the second field are both inductive. This is also valid for electric dipole source and long wire source if the former is far enough from the well and the latter is rather close to it. This point may be discussed in later articles. Assuming the source is located at the coordinate origin (0, 0, 0), the direction is from the inner of the paper to the outside, and Z-axis directs downward. From Maxwell equation, we have the following integral equation:

$$E_y(x, z) = E_y^p(x, z) + \int_S G_E(x, z, x', z') \cdot \sigma_a(x', z') E_y(x', z') \mathrm{d}x' \mathrm{d}z' \quad (1)$$

where E_y is the total electric field, E_y^p is the primary electric field, and G_E is electric Green function. $\sigma_a = \sigma - \sigma_0$ is the difference between conductivity of anomaly body and that of background. S, the region of integral, is the transverse plane of anomaly body. Similarly, we have:

$$H_x(x, z) = H_x^p(x, z) + \int_S GH_x(x, z, x', z') \cdot \sigma_a(x', z') \cdot E_y(x', z') \mathrm{d}x' \mathrm{d}z' \quad (2)$$

$$H_z(x, z) = H_z^p(x, z) + \int_S GH_z(x, z, x', z') \cdot \sigma_a(x', z') \cdot E_y(x', z') \mathrm{d}x' \mathrm{d}z' \quad (3)$$

where G_{Hx} and G_{Hz} is the x direction magnetic Green function and vertical magnetic Green function respectively. Eqns. (2) and (3) may be deduced from Eqn. (1) too. The fields in above three equations have implicit relations to frequency. Eqn. (1) is a typical Fredholm integral equation of the second kind. It is very difficult to inverse σ_a from it because of strong nonlinear nature of the equation. The general method is to replace E_y in the integral with E_y^p, that is, replace the total field with the primary field. This is the basic Born approximation. Then, many kinds of iteration scheme can be employed. However, if conductivity of anomaly body has great differences with that of medium, E_y^p may has great differences with E_y, so the approximation is invalid. Now, we give up this approximation. From Eqns. (1), (2) and (3), we can find the item $\sigma_a E_y$ exists inside the integral in above all three equations. It is just the scattering current J_s. Substituting it into the above three equations, we have:

$$E_y(x, z) = E_y^p(x, z) + \int_S G_E(x, z, x', z') \cdot J_s(x', z') \mathrm{d}x' \mathrm{d}z' \quad (4)$$

$$H_x(x, z) = H_y^p(x, z) + \int_S G_{Hx}(x, z, x', z') \cdot J_s(x', z') \mathrm{d}x' \mathrm{d}z' \quad (5)$$

$$H_z(x, z) = H_z^p(x, z) + \int_S G_{Hz}(x, z, x', z') \cdot J_s(x', z') \mathrm{d}x' \mathrm{d}z' \quad (6)$$

Now we find that: all equations are linear for J_s, and J_s in Eqns. (4), (5) and (6) are the same, so that it can be solved from these three equations simultaneously. In practice, if some components of the field are not obtained, we can use the rest of the equations to solve J_s. After J_s is solved, σ_a is easy to solve. Obviously, the more the observed components and locations, the better the resulted image.

4 EXAMPLES

Suppose a well with 100 m depth is located on the equator plane of source and is 100 m far from it. The background conductivity is 0.001 S/m, the anomalous conductivity is 0.1 S/m, the contrast is $O = 1 - \sigma_a/\sigma_0 = -99$. Divide the image region into 5 m × 5 m grids. Consider the reality of field, the horizontal magnetic field H_x is observed on the surface, the vertical magnetic field H_z is observed in the well. There are totally 121 measuring sites. The frequency of the source signal is 50 kHz. The inverted image by our algorithm is as follows (see Fig. 2, Fig. 3).

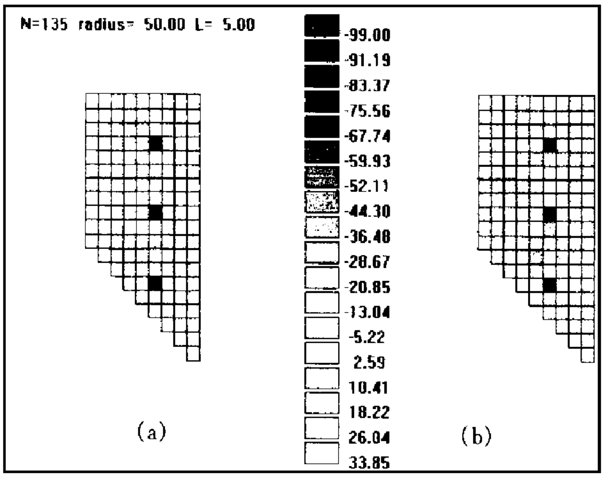

Fig. 2 Model 1 and imaging results

(a) —model; (b) —imaging results

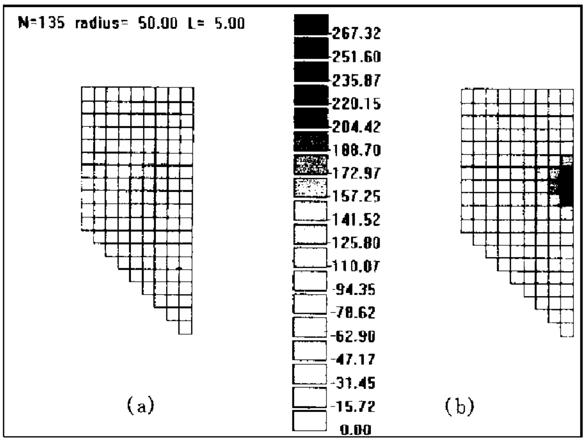

Fig. 3 Model 2 and imaging results

(a) —model; (b) —imaging results

Fig. 2(a) and Fig. 3(a) show the model, and Fig. 2(b) and Fig. 3(b) show the imaging results. Due to the surface-to-well geometry, our imaging region is a rectangle without one corner. Fig. 2(b), showing the contrast of conductivity, gives very well results. On the figure, the deep image has a little distortion due to the weak signal in deep area. Fig. 3 has some differences with Fig. 2. In Fig. 3, we have added 10% Gauss noise to the surface data, 1% Gauss noise to the in-well data. The noise is so strong that almost all kinds of image algorithm will fail. Our two step algorithm is not excepted too. However, here we only implement one step of our algorithm that is only inverse scattering current. Then we calculate the module of the scattering current, and show the results in Fig. 3(b). To compare the results with the gray density plot of the model, we multiple the module by a factor − 99. Now, we find that although we cannot obtain the precise image, we have obtained a significant result. This is very inspirited. The image is biased to right. It may be interpreted, since the source is on the left.

5 CONCLUSION

Through discussion above, a new electric imaging scheme has been supposed, a two step imaging algorithm without any approximation has been put forward. They work very well in simulating results.

REFERENCES

1 Wilt M, Alumbaugh D L, Morrison H F *et al*. Geophysics, 1995, 60: 871− 885.

2 Zhou Q, Becker A, Morrison H F. Geophysics, 1993, 58: 482− 495.

3 Alumbaugh D L, Morrison H F. Geophysics, 1995, 60(3): 846− 870.

4 Newman G A. Geophysics, 1995, 60: 899− 911.

5 Habashy *et al*. J Geophys Res, 1993, FEB10: 1759 − 1775.

6 Torres-Verdin C, Habashy T M. In: Proceedings of 63rd Annual Internat. Mtg Soc Expl Geophys Expanded Abstracts, 1993: 351− 354.

(Edited by He Xuefeng)